A simple method based on routine observations to nowcast down-valley flows in shallow, narrow valleys

Gert-Jan Duine*

Laboratoire d'Aérologie, University of Toulouse, CNRS, France

Laboratoire de Modélisation des Transferts dans l'Environnement, CEA Cadarache, France

Thierry Hedde

Laboratoire de Modélisation des Transferts dans l'Environnement, CEA Cadarache, France

Pierre Roubin

Laboratoire de Modélisation des Transferts dans l'Environnement, CEA Cadarache, France

Pierre Durand

Laboratoire d'Aérologie, University of Toulouse, CNRS, France

Corresponding author address: Laboratoire d'Aérologie, University of Toulouse, 14 Av. Edouard Belin, Toulouse, France.

E-mail: gertjan.duine@gmail.com

ABSTRACT

A simple relation to diagnose the existence of a thermally driven down-valley wind in a shallow (100 m deep) and narrow (1 - 2 km wide) valley based on routine weather measurements has been determined. The relation is based on a method which has been derived from a forecast verification principle. It consists in optimizing a threshold of permanently measured quantities to nowcast the Cadarache (southeastern France) down-valley wind. Three parameters permanently observed at a 110-m high tower have been examined: the vertical temperature difference (between 110 m and 2 m), the wind speed at 110 m and a bulk Richardson number. The thresholds are optimized thanks to the wind observations obtained within the valley during the field experiment KASCADE, which was conducted in the winter of 2013. The highest predictability (correct nowcasting ratio of 0.91) was found for the temperature difference at a threshold value of 1.5°C (or 2.6°C for potential temperature). The applicability of the method to other heights (2 and 30 m) and to summer conditions is also demonstrated. This allowed a reconstruction of the climatology of the down-valley wind which demonstrates that the wind exists throughout the year, and is strongly linked to nighttime duration. This threshold technique will allow to forecast the subgrid-scale down-valley wind from operational numerical weather coarse grid simulations by means of statistical downscaling.

1. Introduction

Under clear skies and weak synoptic forcing, stable stratification develops during the night. Due to surface radiative heat loss, the air layer close to the ground becomes denser than the layer above (Stull 1988). Over sloping terrain a horizontal temperature gradient forms and the air will start to flow downslope as a consequence of negative buoyancy (Manins and Sawford 1979; Haiden and Whiteman 2005). The valley and drainage winds appearing on scales from meters (Mahrt et al. 2001) to tens of kilometers (Jiménez and Cuxart 2014) have been studied all over the globe (Barry 2013). The down-valley flows are mostly independent of above-valley wind conditions (Whiteman and Doran 1993), especially in narrow valleys. They have been documented in climatological studies for valley systems at different scales (Stewart et al. 2002), or categorized as a combination of several parameters, such as net radiation, cooling rate and a temperature difference (Gudiksen 1989; Amanatidis et al. 1992).

Local measurements and observational analyses of down-valley flows remain necessary due to distinct valley geometries and their influences on the flow pattern (Atkinson 1995; Sheridan et al. 2014), especially under stable stratification conditions where pollutant concentration can be highest due to weak dilution. Methods to analyze and predict the down-valley flow characteristics by means of observations have been developed to a large extent, in the form of a radiation Richardson number (Mahrt et al. 2001) or a temperature difference on the vertical (Amanatidis et al. 1992). Drainage depths are determined by means of ambient wind conditions (Barr and Orgill 1989) or with a combination of ridge top wind speed and strength and depth of the inversion (Horst and Doran 1986). However, the studies devoted to predict the down-valley flows are mostly based on observations which are rarely available on a routine basis.

The KASCADE-campaign has been conducted in southeastern France during the winter of 2013 and revealed the dominant existence of a down-valley flow in a shallow and narrow valley, the Cadarache Valley (CV - Duine et al. 2015). This Cadarache down-valley (CDV) wind has been characterized as a thermally driven wind. It occurs mostly during stable stratification periods and is restricted to the valley depth, which is around 100 m. Many facilities of the Cadarache site, one of the research centers of the Commissariat à l'Energie Atomique et aux Energies Alternatives (CEA), lay in the CV, and could potentially emit pollutants in the atmosphere. No measurements are available on a routine basis at the height and location of this CDV wind, but its conditions of existence are to be known for risk management purposes.

Consequently, a methodology has been developed using a dichotomous forecast verification principle (Wilks 2011) to optimize a threshold, enabling to nowcast the down-valley flow presence or absence. As within narrow valleys local meteorology and cold pools can be dominant and do not always reflect the regional meteorology, this method could be generally applied, although its performance highly depends on the valley geometry. To verify the method, a combination of permanent and temporary measurements has been used. From the permanently installed 110 m tower, three potential quantities to nowcast the down-valley flow are available: a vertical temperature difference (between the top of the tower and 2 m), the wind speed at the top of the tower and a combination of the previous two data in the form of a bulk Richardson number. For validation, a temporarily installed mast in the valley is used, equipped with sonic anemometers at three levels from which the CDV wind can be characterized. This 30-m high tower has been deployed during the KASCADE campaign and enabled continuous observations of the valley winds in the CV. The computed thresholds are evaluated at the three several levels and for different seasons.

The paper is organized as follows. In Sects. 2a and 2b the measurement strategy and the general wind behavior in the CV observed during the KASCADE-campaign are explained. The method-

ology to optimize the threshold is presented in Sect. 2c and the candidates for down-valley wind predictors are introduced in Sect. 2d. Results for the optimized thresholds are given in Sect. 3. The choice for the best predictor, its applicability to different heights of the CDV wind and to seasons other than winter is discussed in Sect. 4. Applications of this threshold methodology including a 5-year climatology are given in Sect. 5, and final conclusions and perspectives are given in Sect. 6.

2. Site, observations and methodology

a. Valley description and measurement set-up

The CV constitutes the main part of the Cadarache site (Fig. 1). The valley axis is indicated by the red arrow pointing downslope. Its length is around 6 km until it meets the Durance Valley which is much larger and oriented almost perpendicularly to the CV. The CV is shallow (100 m) and narrow (1 - 2 km), which leads to an aspect ratio (valley depth to its width) of 0.04. The average slope along the valley bottom is 1.2°, whereas the slope of the sidewalls is estimated at around 6°. The land use in the valley is a mixture of deciduous forest, grass, buildings and artificial surfaces, but grass dominates in the valley bottom and deciduous forest on the sidewalls.

Two measurement towers deployed during KASCADE are used in this study: the permanently installed 110-m high tower at La Grande Bastide (GBA) and the 30-m flux tower (M30), installed for the campaign duration only. Both towers are situated on the axis of the CV, the GBA near to the lower end, and the M30 halfway of the valley length. The GBA-tower is only equipped with sensors at its top and bottom: wind and temperature are measured at 110 m, and temperature at screen level (2 m). The top level of the GBA-tower is situated above the CV sidewalls and therefore does not experience the inside-CV processes. M30 was instrumented with sonic anemometers at

heights of 2, 10 and 30 m. A full list of the other M30-sensors, and other details and results of the campaign can be found in Duine et al. (2015).

b. Wind behavior in the Cadarache Valley

The flow within a valley has been related to the above-valley wind conditions by Whiteman and Doran (1993) who classified this relationship into four types: thermally driven, downward momentum transport, forced channeling and pressure driven channeling. These relationships are indicated by the lines in Figs. 2a to 2c, after adaptation to the CV orientation, i.e. SE for down-valley winds and NW for up-valley winds. The behavior of our observations with respect to this theoretical framework is presented in Fig. 3, which shows the wind direction measured within the CV at 10 m from the M30 tower and above the valley at 110 m from the GBA tower. Figure 3a shows the occurrences of the wind direction at 110 m, with a classification of the wind origin on the mesoscale. The three lower pictures show inside valley (M30) against above-valley wind directions (GBA). They all show the same data but are further classified with respect to a threshold defined either on the wind speed at 110 m at GBA U_{110m} (Fig. 3b), or the atmospheric stratification as characterized by the temperature difference ΔT between 110 and 2 m at GBA (Fig. 3c), or a bulk Richardson number Ri_B (Fig. 3d):

$$Ri_B = \frac{g \cdot (\Delta T + \Gamma_d \Delta z) \cdot \Delta z}{T_{110m} \cdot (\Delta U)^2} \tag{1}$$

with g being the gravitational acceleration of 9.81 m s^{-2} and Γ_d the dry adiabatic lapse rate of 9.8 K km^{-1} for potential temperature calculation. Δz corresponds to the height difference between the temperature measurements. The usage of Ri_B to our purpose is further detailed in Sect. 2d. The classifications used in the figure are used as a first step in the analysis to describe the important features of the valley adapted to the theoretical framework presented in Fig. 2. The fixed

thresholds are arbitrarily chosen and relatively simple, i.e. an arbitrary wind speed threshold, stable vs. unstable conditions and turbulent vs. laminar regime. Picking up the theoretical framework of Whiteman and Doran (1993) from Fig. 2 and the combination with our measurements (Fig. 3), enables to determine under which conditions the CDV wind develops.

The first group given in Whiteman and Doran (1993) classification of valley winds is a thermally driven flow, which has an upslope direction during the day, and a downslope direction in the night. This theoretical relationship is indicated in Fig. 2a. Typically, the thermally driven flow is fully independent of above-valley wind conditions. It is especially observed during weak synoptic forcing in combination with clear skies. Relatively narrow valleys like the CV favor the existence of thermally driven flows during such conditions. Figure 3 reveals that during low wind speed conditions (Fig. 3b) or stable periods (Fig. 3c and Fig. 3d) there is a high preference for a down-valley flow within the CV, as a higher density of blue dots can be observed in the CDV direction. The up-valley channeled wind, i.e. NW wind, presents a much more scattered direction than the CDV wind. There are two possible reasons for that: firstly, the orography SE to the M30 location resembles a well-defined valley, whereas NW flows experience a more complex area, composed of the Durance and Cadarache valleys and local hills, before arriving at the M30 site (see Fig. 1); secondly, up-valley, northwesterly winds are generally observed either during high wind speed events such as a Mistral, or during neutral to moderately stable situations, i.e. conditions with sufficient vertical transfer of momentum to imprint the above-valley wind direction into the CV.

Another origin for valley winds is identified by Whiteman and Doran (1993) as downward momentum transport. For this relationship, the flow within the valley is totally dependent on the above-valley wind. The theoretical relationship is indicated by the diagonal line in Fig. 2a. It is favored by a wide valley (Whiteman and Doran 1993) and can be mostly observed during unstable and neutral conditions. Such situations are highlighted by the red dots for either high wind speeds

(Fig. 3b) or unstable conditions (Figs. 3c and 3d). In the CV, downward momentum transport occurs mostly for SE and NW upper winds, as the highest occurrences are found in these quadrants. The westerly directions are mostly measured during daytime, when instability is causing upslope anabatic flows, and/or during Mistral events which have west to northwest directions in the region. The SE-directions are typically observed during cloudy or precipitation events (Duine et al. 2015). Note that the latter conditions cause a direction which is intermingled with the CDV wind, but can be very well distinguished by means of the colors (e.g. red crosses on Fig. 3d).

Two other relationships are indicated by Whiteman and Doran (1993) as forced channeling and pressure driven channeling. Forced channeling (Fig. 2b) is favored during unstable and neutral conditions within narrow valleys (Weber and Kaufmann 1998) while pressure driven channeling (Fig. 2c) typically occurs when moderately stable conditions are dominant in wide and shallow valleys (Carrera et al. 2009). Based on the figures, as the typical relation for forced or pressure-driven channeling are not visible, we conclude that these relationships are non-dominant mechanisms for a CDV wind to develop.

Thus, it is clear that the CDV wind mainly develops during stable conditions and low wind speeds. Although the GBA-tower does not provide wind measurement inside the CV, Fig. 3 reveals the plausibility of a relationship between the GBA-tower measurements and the occurrence of the CDV wind. The objective is now to find an optimal threshold under which the CDV wind can be inferred from GBA-observations only and without any wind measurement in the valley.

c. Procedure for threshold optimization

To optimize a threshold based on the GBA observations, we use a procedure that defines a quality index based on contingency table values. The method is used for verification of non-probabilistic forecasts of bilateral events (Wilks 2011). The principle relies on dichotomous predictors, so by

using a threshold on GBA observations we define a bilateral predictor with which we can nowcast the CDV wind. In our case, the bilateral event is the CDV wind presence or absence. The threshold candidates coming from GBA observations are introduced in the next section.

We define the contingency table (Table 1). The letters a to d in the table are the count of occurrences for each couple of events, i.e. CDV wind observed or no CDV wind observed vs. CDV wind nowcasted or no CDV wind nowcasted. The thermallyd driven CDV wind is diagnosed from M30 observations when the wind direction is in the range [90 - 180°]. A sensitivity study to restrict the down-valley wind to smaller direction ranges, e.g. between 110° and 160°, did not influence the final results. The letters in the contingency table are described as follows:

a) Correct nowcast or hit: A CDV wind is nowcasted and has been observed at M30.

b) False alarm: a CDV wind is nowcasted but has not been observed.

c) Missed nowcast: a CDV wind is not nowcasted, but has been observed.

d) Correct rejection: a CDV wind is neither nowcasted nor observed.

To find the optimal threshold for the predictor criterions given in Table 1 we use the combined counts of the contingency table values by applying two different tests (Wilks 2011)

$$PC = \frac{a+d}{a+b+c+d} \tag{2}$$

$$bias = \frac{a+b}{a+c} \tag{3}$$

where the "Proportion Correct" PC represents the fraction of the total number of events n ($n = a + b + c + d$) for which the threshold correctly classified an event (a) or non-event (d). To optimize the PC, a and d should be as high as possible, and b and c as low as possible. It is a ratio ranging from 0 to 1, the higher the value for PC, the better the threshold-value for a given

criterion. The *bias* is used to evaluate the balance between the number of nowcasted CDV wind events to the number of observed CDV wind events. It is expressed as overnowcasting (>1) or undernowcasting (<1) of the event and should therefore be as close to 1 as possible. Equations 2 and 3 are the framework for choosing an optimized threshold.

All data of the winter of 2013 collected during the KASCADE continuous measurement period are used, i.e. from 13 December 2012 to 16 March 2013. The values are 30-minute averaged. A minimum threshold of 0.5 m s^{-1} is applied to wind speed because for lower wind speeds the wind direction is ill-defined. All values inside the SE-SE quadrant are discarded because this quadrant is blurred with two types of conditions: the stable conditions which favor a thermally driven CDV wind on the one hand and the cloudy weather and precipitation events which typically occur under southeasterly winds (Duine et al. 2015) on the other hand.

d. Threshold candidates

The purpose is to find which measured quantity at GBA can be best used to nowcast the CDV wind. The threshold optimization procedure (see Sect. 2c) is applied to quantities derived from the GBA available measurements:

1) a vertical temperature difference $\Delta T = T_{110m} - T_{2m}$

2) the wind speed at 110 m U_{110m}

3) a combination of ΔT and U_{110m} in the form of a bulk Richardson number Ri_B (see Eq. 1).

The Richardson number is a good indicator for stability, as it relates wind speed to buoyancy and is classically used to assess stability inside air masses. It has been used before as a predictor for shallow drainage flows (Mahrt et al. 2001), with the addition of longwave radiation, which defines a radiation Richardson number. Unfortunately, there are no routine observations of net longwave radiation, thus we must rely on wind speed and a vertical temperature difference only.

Note that we have adapted the classical Ri_B to the availability of observations: humidity measurements at the GBA-site are only available at 2 m. Thus, we cannot determine a virtual temperature T_v at 110 m so we must base ourselves on the difference in absolute temperature T alone. The influence of neglecting the humidity variation in Eq. 1 has been checked by tethered balloon measurements which were deployed at location M30 (Fig. 1) during the KASCADE-campaign and showed little difference between the use of T vs. T_v: a relative error of around 2% on Ri_B is determined. The Ri_B increment used for optimization was taken as 0.1 and so in the range of interest for Ri_B (i.e. -1 to 5) the moisture-related error is lower than this increment and therefore does not affect the result. Furthermore, wind speed observations are only available at the height of 110 m. Consequently, we will assume that $U(2m) = 0$, so that $\Delta U \sim U_{110m}$. This assumption is probably not a major source of error, because a study of the GBA site characteristics, based on wind profiles from a SODAR and two measurement stations at the Cadarache site, has shown that the roughness length z_0 is 1.03 m and the zero-plane displacement height is of the order of 5 m. The 2-m level is therefore in the local roughness sub-layer, whereas the 110-m level observations are representative of a much larger area.

3. Results

a. Threshold ΔT_T

The contingency table values of *PC* and *bias*, as defined in Table 1 and in Eqs. 2 and 3, are presented in Figs. 4a and 4b for the temperature difference ΔT varying in the range -3 to 9°C by increments of 0.1°C. The optimized values are given in Table 2.

A maximum score of 0.91 for *PC* is obtained for the temperature difference threshold ΔT_T=1.5°C (vertical dashed line in both pictures). The value of ΔT_T represents the best separation value for

which a thermally driven CDV wind (i.e. not thermally driven) is nowcasted when $\Delta T > \Delta T_T$ or a non-CDV wind is nowcasted if $\Delta T < \Delta T_T$. The high value for *PC* at ΔT_T reflects the relevance of the criterion and the threshold chosen. It further indicates that ΔT_T is a good candidate for this procedure. This is emphasized by the small but relatively high peak of the *PC* curve. This threshold is a rather safe one, as *PC* drops quickly when the value is set at higher or lower temperature differences. The skill of the optimum threshold is further reflected in the *bias* of 1.03, which is very close to 1, the optimal value. The ratio of missed events $b + c$ is 0.09, see Sect. 4a for more details.

The value of 1.5°C corresponds to a potential temperature difference of approximately 2.6°C. This quite high value confirms that the wind inside CV is primarily thermally driven and can be linked to very stable situations.

b. Threshold U_T

The second criterion under investigation to nowcast the CDV wind is based on the wind speed at 110 m. The same procedure is followed as for ΔT_T (Sect. 3a) with increments of 0.1 m s^{-1} in the range 0.5 m s^{-1} to the maximum observed wind speed. The results are shown in Fig. 5 and Table 2.

We find an optimal threshold for U_T at 4.0 m s^{-1}, with a *PC* of 0.72. This is the highest score at which a separation can be made to nowcast either a thermally driven CDV wind ($U < U_T$) or a non-CDV wind ($U > U_T$). The maximum value for *PC* based on U_{110m} is lower than based on ΔT_T. It indicates that a threshold based on wind speed is not as good as when using ΔT_T as a CDV wind predictor. The respective higher and lower counts for false alarm b and correct rejection d (Table 2) point out why the skill is lower for U_T than for ΔT_T. Besides, at the optimal threshold, the false alarm value b is 4 times higher than the missed value c. This indicates that a CDV

wind is nowcasted too leniently, which is also reflected in the *bias*-value of 1.43, translating as an overforecast of the event. Note also that the peak for *PC* is flatter than for ΔT_T, which means that using U_T alone as a predictor for the CDV wind is not an indisputable method. Overall, the wind speed at 110 m does play a role in the existence of a CDV wind, but is not as relevant as the vertical temperature difference.

c. Threshold Ri_{B_T}

The last quantity we check is the bulk Richardson number Ri_B (Eq. 1). The results are shown in Fig. 6 and Table 2. A *PC*-score of 0.86 is found at the threshold $Ri_{B_T} = 0.8$. The corresponding *PC*-value of 0.86 is high, but still lower than for ΔT_T. It is remarkable that the *PC*-value sharply rises when passing the zero-line of Ri_B, confirming the fact that the CDV wind is indeed strongly related to stability. The values of *PC* at the right side of the peak are relatively high with respect to the peak value itself, which is an extra indication that the *Ri*-criterion may work less good. At the threshold-value of Ri_B, the number of false alarms b is twice as large as missed classifications c (Table 2). Therefore, the optimal threshold Ri_{B_T} of 0.8 results in some overnowcasting of the CDV wind, as is also indicated by the quite high value of the *bias* (1.15).

The value of $Ri_{B_T} = 0.8$ is a little lower than the threshold value of 1.0 which theoretically marks the transition from turbulent to non-turbulent regime in stable conditions. It is difficult to ascertain whether the difference between these two values is significant, because the height range in which Ri_B is computed is quite large (108 m), and the uncertainty on *Ri*-estimates through a 'bulk' assumption increases with the thickness of the layer, especially close to the surface where the vertical gradients are the highest (Stull 1988). Furthermore, another reason of the lesser success for Ri_{B_T} than for ΔT_T may lie in the hysteresis behavior of critical *Ri*-thresholds, i.e. different

values when passing from laminar to turbulent regime or vice versa (McTaggart-Cowan and Zadra 2014). In this study, both transitions are mixed, and so could lower the score.

4. Discussion

a. Choice of the predictor

The temperature difference threshold proved to be the best predictor of CDV winds. The *PC*-value of 0.91, which is close to, but somewhat lower than 1, means that some events are badly nowcasted. In this section we try to find out for which types of conditions the ΔT_T-criterion fails.

Figures 7a and 7b illustrate the performance of the temperature threshold to nowcast the CDV wind: in Fig. 7a, only the data for which the condition is valid ($\Delta T > 1.5°$C) are shown. The result is compared to the actually observed winds at 10 m in the CV. The data falling outside the CV direction ($135° \pm 45°$), i.e. for which the nowcast fails, are plotted on the gray-shaded areas, whereas the successful data fall in the white area. On the contrary, in Fig. 7b the data for which the condition is not valid are plotted. The gray and white area are thus reversed with respect to Fig. 7a, with the exception of the CDV wind conditions inside as well as above the CV. This is because, in this case, the observed wind with a SE-direction at 10 m is due to the momentum transfer from the above-valley wind (see Fig. 2 and Fig. 3d), and not to the stability conditions. Furthermore, the data are sorted according to the hour of the day. In Figs. 7c and 7d, the same plots are shown as in Figs. 7a and 7b, but the data are sorted according to the wind speed at 110 m. During the period of measurement, sunsets were in the range 05:40 and 07:02 UTC, and sunrises between 16:00 and 17:48 UTC.

By applying ΔT_T of 1.5°C we miss 9% of the thermally driven CDV wind events and the non-CDV wind events. The false alarms (i.e. $\Delta T_T > 1.5°$C and no CDV wind observed) have to

be analyzed according to the wind speed: wind speeds higher than 4 m s^{-1} occur mainly in the NW-NW quadrant and are found during nighttime periods. These valley winds are related to downward momentum transport where turbulent motions are transported downwards (hence, Fig. 2). As such they oppose the onset of stability and so the formation of a CDV wind. Wind speeds lower than < 4 m s^{-1} are mostly observed during the morning and evening transitions. Here stable stratification has already developed on the GBA-site close to the surface, but the down-valley wind at M30 has not set yet (during evening transition), or the stability at GBA is still present, but the down-valley jet has already been eroded (morning transition). To conclude, for a thermally driven CDV wind nowcast, one should be careful at applying the threshold when the wind speed at GBA is higher than 4 m s^{-1} and accompanied by a northwesterly direction.

On the other hand, missed nowcasts occur primarily during low wind speed conditions at 110 m (i.e. < 4 m s^{-1}) and, although these misses have been observed throughout the full 24-hour period of the day, they are mostly frequent during the sunrise transition period.

b. Wind prediction at other heights

The tethered balloon observations during the KASCADE campaign have shown that the CDV wind can frequently grow up to a height of 50 m (Duine et al. 2015). In addition to the 10 m height, sonic anemometers were also installed at 2 and 30 m so the validity of the threshold can also be checked at these heights. This is done by applying the same procedure as for the 10 m CDV wind. At the 2 m level however, due to equipment malfunctioning, the dataset is 3 weeks shorter.

At 2 m comparable values for *PC* (0.91) and *bias* (1.04) are found, but for a slightly higher ΔT-value of 1.6°C (Fig. 8 and Table 3). At 30 m the optimal score for *PC* is also shifted to a ΔT-value of 1.6°C, but with a score of 0.87 and a *bias* of 1.04. However, due to the flatness of the *PC* peak, we can consider the threshold on ΔT is identical for the three heights.

c. Summer conditions

A mobile 2-m wind mast has been installed in the CV from 18 July to 25 September 2014 on M30 site so we can check the validity of the ΔT threshold at 2 m (1.6°C) during summer conditions.

The results (Table 3) show that the CDV wind can be forecasted in summer as well and confirms the general applicability of the index. Interestingly, in spite of approximately the same sample size (2002 observations during summer vs. 1946 during winter) the number of *a* (good hits) events occurred half as often as in winter. In summer, this event is mostly replaced by correctly rejected events (*d*: non-CDV wind and ΔT <1.6°C) and sometimes by false alarms (*b*). Therefore, the high value of *PC* comes from a high number of up-valley winds being correctly classified ($\Delta T <$ 1.6°C). Note that more than 72% of the values are below the threshold in summer, whereas this is 58% for winter conditions (ratio (*c*+*d*)/*n*). Non-thermally driven CDV wind observations ((*b*+*d*)/*n*) are less frequent in winter (59%) than in summer (78%). A connection to the respective length of day and night for valley winds is worth considering (Giovannini et al. 2015) and could be checked on a year-long sample in the next section.

5. Climatology of ΔT_T

The previous sections have shown the general applicability of the vertical temperature difference at GBA to nowcast the CDV wind by means of the GBA-tower observations with a relatively low uncertainty. The GBA-tower has been installed for many years already and a long-term dataset is available.

We apply the ΔT_T threshold of 1.5°C to obtain a climatology for thermally driven CDV wind occurrences at 10 m, for the years 2007 to 2011. Figure 9 shows monthly statistics on CDV wind and non-CDV wind occurrences. During the winter months, values of ΔT favoring a CDV wind

are present almost half of the time and shows that the CDV wind is a dominant wind in winter. The occurrence diminishes gradually to a minimum in June, where conditions favoring thermally driven downslope winds are present during a third of the time. Consequently, the occurrence of this wind is strongly related to the length of the night which confirms the conclusion of Sect. 4c.

The occurrences of the temperature threshold for the KASCADE period (December 2012 - March 2013) are also shown in Fig. 9. Note that the measurement period for KASCADE in December and March has been approximately only half of the month. Against the climatology reconstructed for 2007 - 2011, the months of December and February in particular show a higher occurrence of the CDV wind, whereas in January and in March the occurrences of non-CDV winds have been particularly higher.

6. Conclusions & perspectives

A forecast verification principle has been used in a methodology that determines an optimum threshold to nowcast a down-valley wind in a minimally-instrumented shallow valley. The method is able to identify the best performing quantity to nowcast the down-valley winds. The best predictor, a vertical temperature difference, has been tested for different valley wind heights and seasons. Consequently, it can be used as a nowcasting tool for the thermally driven down-valley flow but also to reconstruct the valley climatology, and it can serve as a tool for statistical downscaling in operational forecasting.

To carry out the threshold optimization, temporary observations of the down-valley wind were combined with measurements of a permanently installed 110-m high tower. The observations were taken from the KASCADE-dataset, a field experiment conducted in the winter of 2013 at the Cadarache site in southeastern France. Cadarache, one of the research centers of the CEA, lays along the shallow and narrow (100 m deep, 2 km wide) CV and comprises several facilities

whose operation requires an assessment of atmospheric release dispersion. As in the CV itself no real-time monitoring is available to fully capture the dominant CDV wind, the method presented has been developed to take advantage of the existing instrumentation.

Three quantities have been tested to identify the most reliable predictor; a vertical temperature difference ΔT, a wind speed above the valley walls U_{110m} and a bulk Richardson number Ri_B. For a down-valley wind occurrence at 10 m, the ΔT came out as the best predictor index at a threshold value ΔT_T of 1.5°C, achieving a *PC* of 0.91. It defeats the Ri_B threshold of 0.8 (*PC*=0.86) and U_{110m}-threshold of 4.0 m s^{-1} (*PC*=0.72), and confirms that the CDV wind is primarily thermally driven. Explanations why ΔT_T performs better than Ri_{B_T} in predicting a drainage wind are the large bulk of measurements at the GBA-tower (108 m) and the hysteresis behavior of Ri. However, the applicability of the found optimal threshold is not fully exclusive and needs some caution. For example, when $\Delta T < \Delta T_T$ under weak wind situations, CDV winds could be present. Furthermore, situations when $\Delta T > \Delta T_T$ with high wind speeds during nighttime, or low wind speed conditions around the sunset and sunrise transitions needs caution as well.

In addition to the 10 m wind nowcast, ΔT_T has been optimized for 2 and 30 m CDV winds. Similar values were found for the temperature difference: 1.6°C, with high values for *PC* of 0.91 and 0.87, respectively. A comparison with available measurements at 2 m in the summer of 2014 confirmed the found threshold value at this height, and so approved the general applicability of this threshold throughout the year. By means of the long-lasting availability of temperature measurements at the GBA-tower, a 5-year climatology could be made based on the found threshold, and revealed the existence of the thermally driven CDV wind throughout the year. Its occurrence is largely dependent on the night length. It further showed the relative importance of strong stability during the December and February months of the KASCADE-campaign.

Finding that a high-score nowcasting can be achieved through the use of only three routinely accessible parameters is of great practical importance for impact assessment and local risk management of pollutant dispersion. Moreover, daily operational forecasts are necessary for sanitary and safety purposes. However, the current operational forecasts are calculated with meteorological models on a relatively coarse grid (i.e. 1 - 3 km) which do not resolve the small valleys as the CV and so do not meet the requirement to forecast thermally driven down-valley winds at such small scales. In this instance, the identification of the vertical temperature difference as a threshold to nowcast the down-valley wind opens perspectives to forecast it by completing dynamical simulations with the statistical downscaling illustrated by this method.

Acknowledgments. This work has been funded by the CEA in the form of a PhD-grant and the financing of the KASCADE-campaign. Laboratoire d'Aérologie are acknowledged for the provision of measurement material during the campaign.

References

Amanatidis, G., K. Papadopoulos, J. Bartzis, and C. Helmis, 1992: Evidence of katabatic flows deduced from a 84 m meteorological tower in Athens, Greece. *Bound.-Lay. Meteorol.*, **58 (1-2)**, 117–132.

Atkinson, B., 1995: Orographic and stability effects on valley-side drainage flows. *Bound.-Lay. Meteorol.*, **75 (4)**, 403–428.

Barr, S., and M. M. Orgill, 1989: Influence of external meteorology on nocturnal valley drainage winds. *J. Appl. Meteorol.*, **28 (6)**, 497–517.

Barry, R. G., 2013: *Mountain weather and climate, 3rd edition*. Cambridge University Press, 506 pp.

Carrera, M. L., J. R. Gyakum, and C. A. Lin, 2009: Observational study of wind channeling within the St. Lawrence River Valley. *J. Appl. Meteorol. Clim.*, **48 (11)**, 2341–2361.

Duine, G.-J., T. Hedde, P. Roubin, P. Durand, M. Lothon, F. Lohou, P. Augustin, and M. Fourmentin, 2015: Valley-driven flows in stable stratification - Observations in a complex orography area during the KASCADE field experiment. *submitted to Q. J. Roy. Meteor. Soc.*

Giovannini, L., L. Laiti, D. Zardi, and M. de Franceschi, 2015: Climatological characteristics of the Ora del Garda wind in the Alps. *Int. J. Climatol.*, doi:10.1002/joc.4270.

Gudiksen, P. H., 1989: Categorization of nocturnal drainage flows within the Brush Creek Valley and the variability of sigma theta in complex terrain. *J. Appl. Meteorol.*, **28 (6)**, 489–495.

Haiden, T., and C. D. Whiteman, 2005: Katabatic flow mechanisms on a low-angle slope. *J. Appl. Meteorol.*, **44 (1)**, 113–126.

Horst, T., and J. Doran, 1986: Nocturnal drainage flow on simple slopes. *Bound.-Lay. Meteorol.*, **34 (3)**, 263–286.

Jiménez, M. A., and J. Cuxart, 2014: A study of the nocturnal flows generated in the north side of the Pyrenees. *Atmos. Res.*, **145**, 244–254.

Mahrt, L., D. Vickers, R. Nakamura, M. Soler, J. Sun, S. Burns, and D. Lenschow, 2001: Shallow drainage flows. *Bound.-Lay. Meteorol.*, **101 (2)**, 243–260.

Manins, P., and B. Sawford, 1979: A model of katabatic winds. *J. Atmos. Sci.*, **36 (4)**, 619–630.

McTaggart-Cowan, R., and A. Zadra, 2014: Representing Richardson Number Hysteresis in the NWP Boundary Layer . *Mon. Wea. Rev.*, **143 (4)**, 1232–1258.

436 Sheridan, P., S. Vosper, and A. Brown, 2014: Characteristics of cold pools observed in narrow
437 valleys and dependence on external conditions. *Q. J. Roy. Meteor. Soc.*, **140 (679)**, 715–728.

438 Stewart, J. Q., C. D. Whiteman, W. J. Steenburgh, and X. Bian, 2002: A climatological study of
439 thermally driven wind systems of the US Intermountain West. *B. Am. Meteorol. Soc.*, **83 (5)**,
440 699–708.

441 Stull, R. B., 1988: *An Introduction to Boundary Layer Meteorology*. Kluwer Academic Publishers,
442 666 pp.

443 Weber, R. O., and P. Kaufmann, 1998: Relationship of synoptic winds and complex terrain flows
444 during the MISTRAL field experiment. *J. Appl. Meteorol.*, **37 (11)**, 1486–1496.

445 Whiteman, C. D., and J. C. Doran, 1993: The relationship between overlying synoptic-scale flows
446 and winds within a valley. *J. Appl. Meteorol.*, **32 (11)**, 1669–1682.

447 Wilks, D. S., 2011: *Statistical methods in the Atmospheric Sciences*, Vol. 100. Academic press,
448 676 pp.

LIST OF TABLES

TABLE 1. Contingency table for verification of CDV wind occurrence. See text for the criterions used.

		Wind observations (M30)	
		CDV wind	No CDV wind
Criterion (GBA):	Satisfied	a	b
ΔT, U_{110m} or Ri_B	Not satisfied	c	d

TABLE 2. Optimized threshold values and contingency table values for the candidate criterions.

Type	ΔT	U_{110m}	Ri_B
Threshold unit	[°C]	[m s^{-1}]	[-]
Height [m]	10	10	10
Season	winter	winter	winter
Threshold	**1.5**	4.0	0.8
PC	**0.91**	0.72	0.86
Bias	**1.03**	1.43	1.15
a	1011	993	1029
b	141	601	273
c	109	144	108
d	1401	961	1289
n	2662	2699	2699

456 TABLE 3. *PC*, *bias* values, and contingency table of ΔT criterion for three different heights in winter and at 2
457 m in summer.

Height [m]	10	30	2	2
Season	winter	winter	winter	summer
Threshold [°C]	1.5	1.6	1.6	1.6
PC	0.91	0.87	0.91	0.87
Bias	1.03	1.12	1.04	1.27
a	1011	926	708	372
b	141	250	104	185
c	109	120	76	67
d	1401	1513	1058	1378
n	2662	2809	1946	2002

LIST OF FIGURES

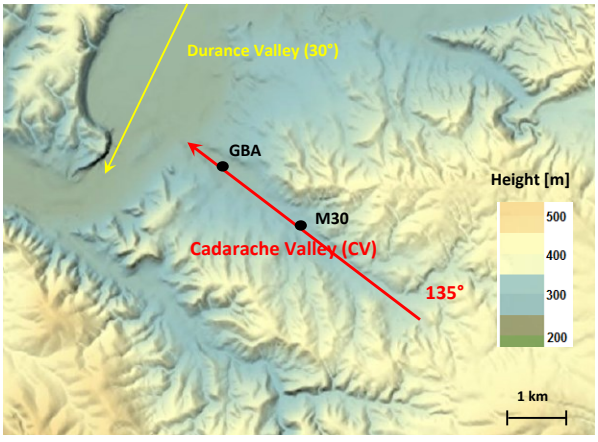

FIG. 1. The Cadarache Valley (CV) and the middle Durance Valley. The red line indicates the CV axis orientation and length. The downslope directions of the bottom of the two valleys are marked by the arrow heads. The 110-m high tower La Grande Bastide (GBA) and the 30-m high tower M30 are both on the axis of the CV. Source: Geoportail.gouv.fr (IGN).

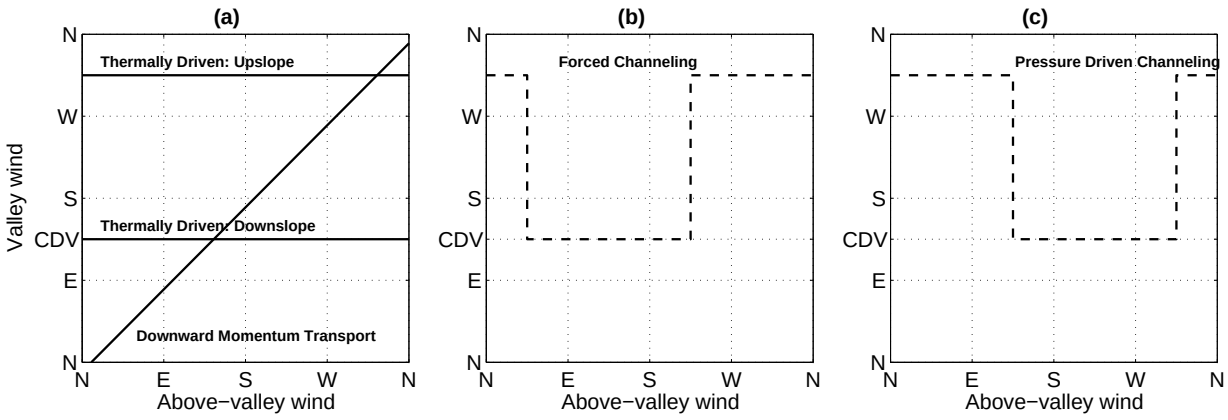

FIG. 2. Inside-valley wind direction against above-valley wind direction according to Whiteman and Doran (1993), adapated to the CV. The direction for the Cadarache down-valley (CDV) is indicated on the y-axis. The different configurations are split in three diagrams (a, b and c) for a better legibility.

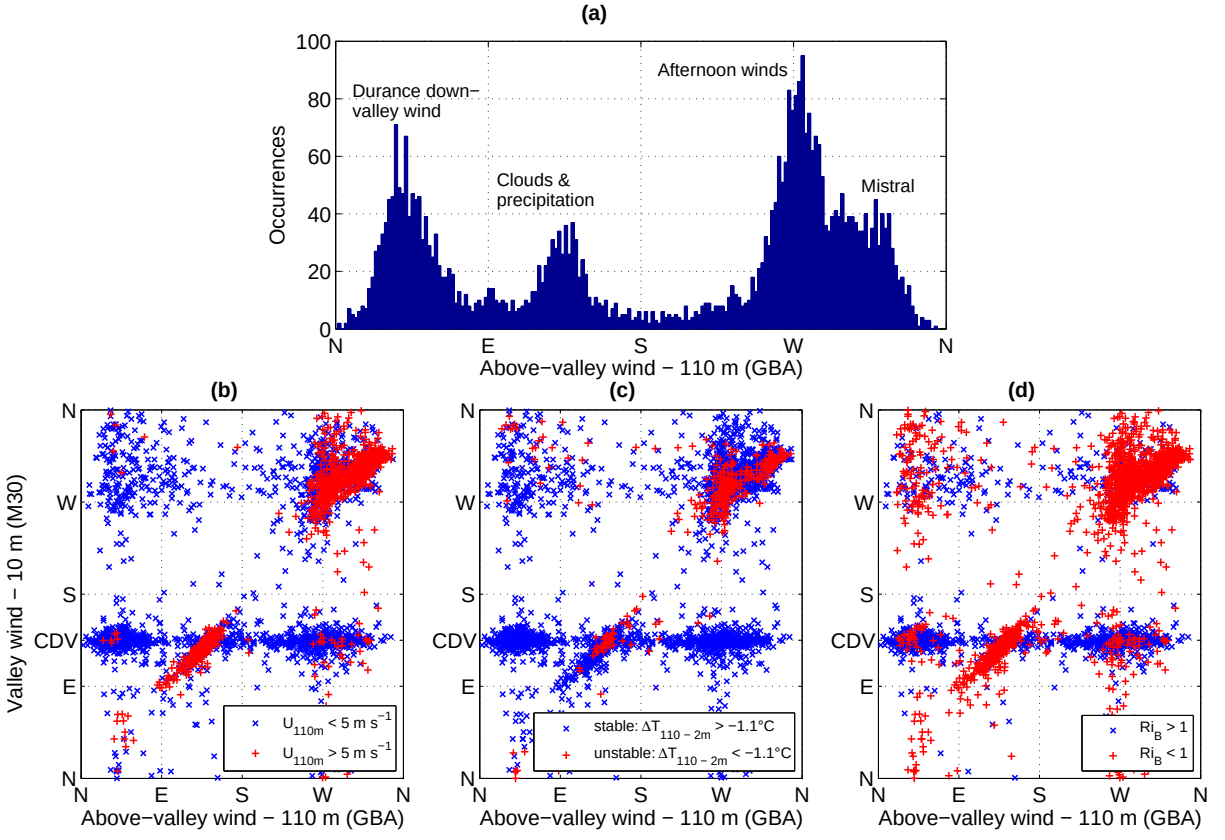

498 FIG. 3. (a) Above-CV wind direction occurrence measured at 110 m, and (b) to (d): wind direction in the CV
499 at 10 m against the above-valley wind direction at 110 m, divided into two classes according to threshold values
500 (defined in the text). Data is from 13 December 2012 to 16 March 2013.

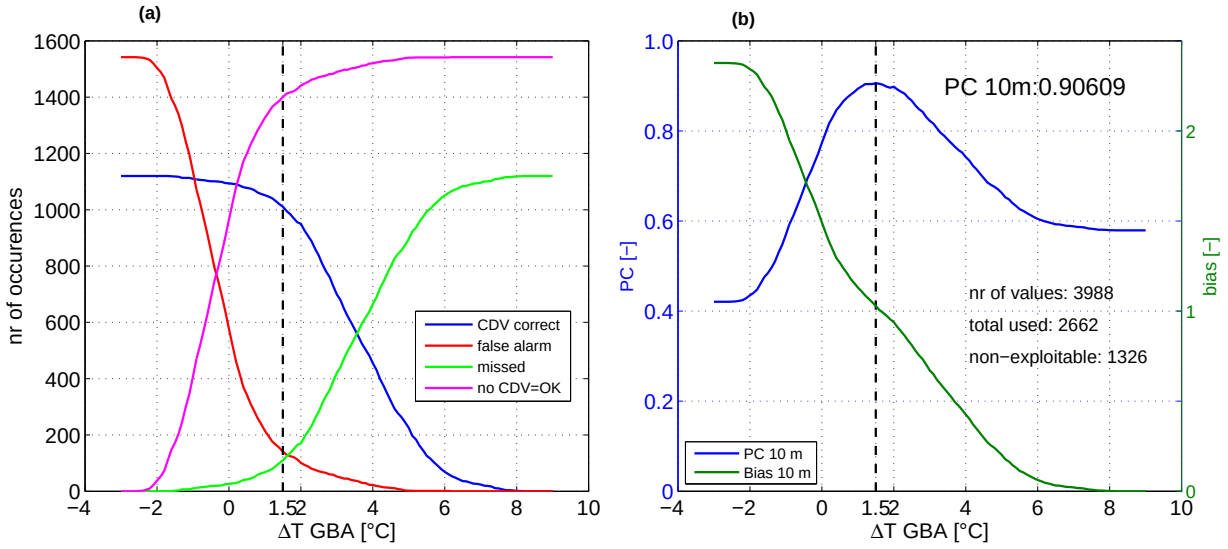

FIG. 4. (a) Contingency table values for the different events as defined in Table 1, calculated for the ΔT criterion and (b) values of *PC* (blue line, left scale) and *bias* (green line, right scale). The vertical dashed lines indicate the threshold value for which the best score is obtained. Data from 13 December 2012 to 16 March 2013.

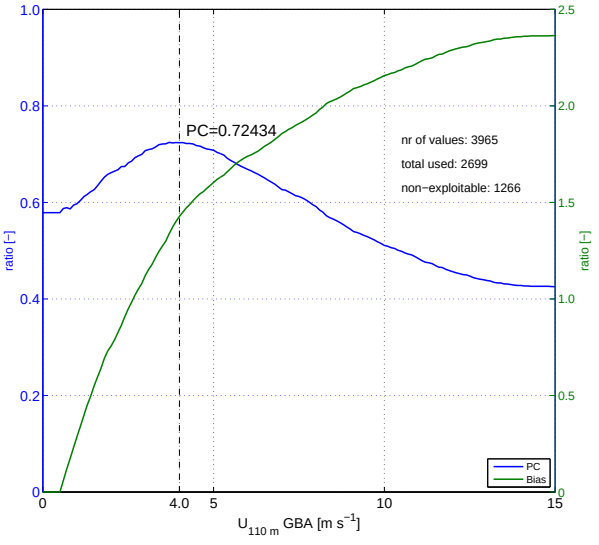

505 FIG. 5. Same as Fig. 4b but for a criterion based on 110 m wind speed measurements at GBA. The optimal
506 threshold is found at 4.0 m s^{-1}. Data from 13 December 2012 to 16 March 2013.

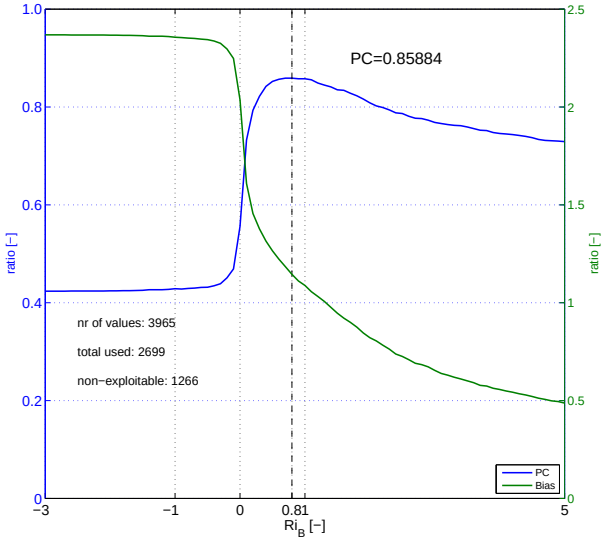

FIG. 6. Same as Fig. 4b but for an optimization by means of a bulk Richardson number. The optimal threshold is found at 0.8. Data from 13 December 2012 to 16 March 2013.

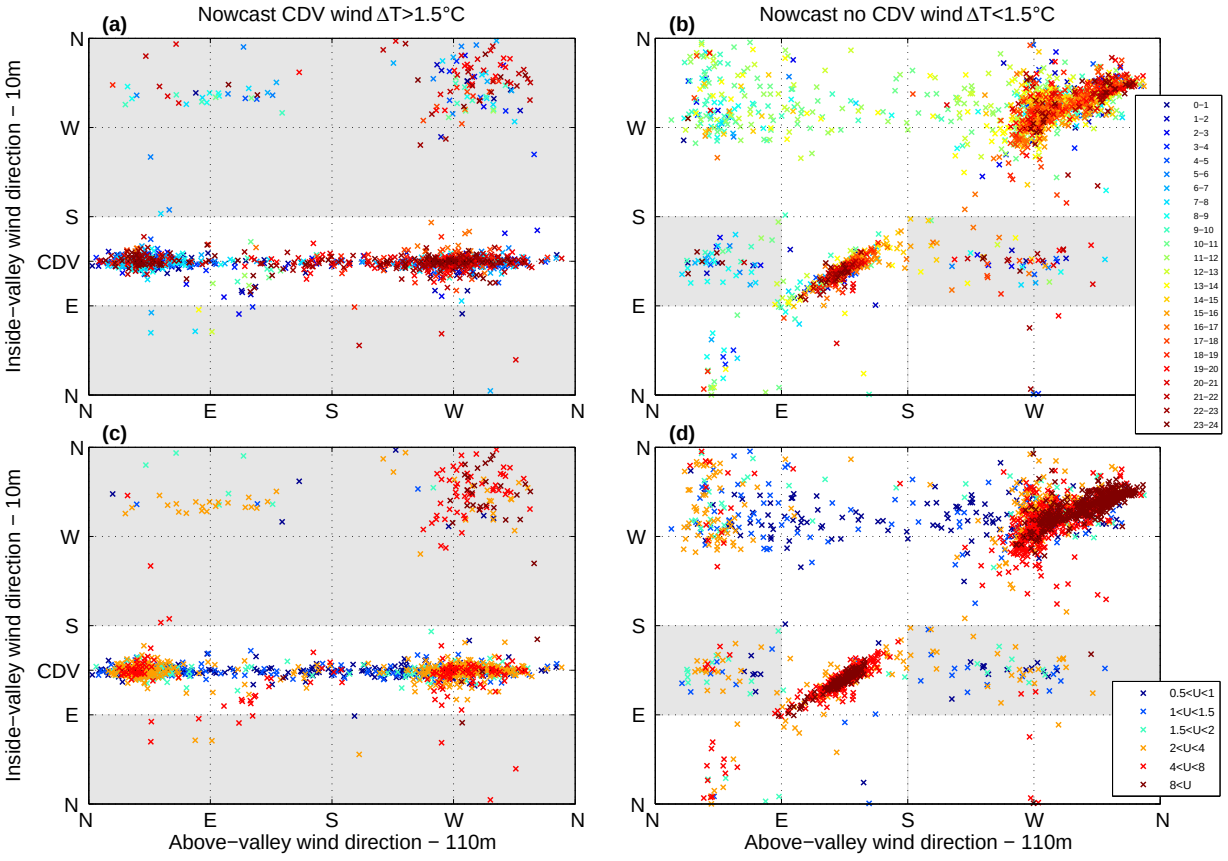

509 FIG. 7. Relation between wind directions inside (10 m) and above (110 m) the valley, according to whether
510 ΔT_T exceeds (left diagrams) or is below (right diagrams) the optimal threshold of 1.5°C. In the two upper
511 diagrams (a and b), the plots are sorted according to the hours (UTC) and in the two lower diagrams (c and d)
512 according to the wind speed observed at 110 m. White and gray backgrounds denote good and bad nowcast,
513 respectively. The color scales on the right textboxes are also valid for the corresponding left diagram. Data from
514 13 December 2012 to 16 March 2013.

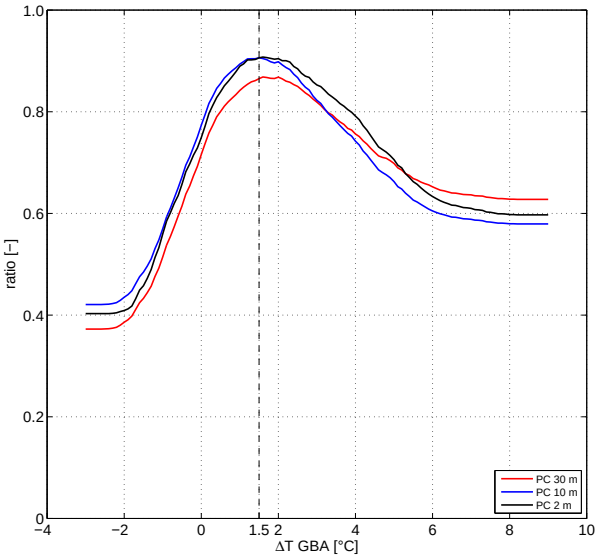

FIG. 8. Same as Fig. 4 but for the other two measurement heights, 2 m (in black) and 30 m (in red). For comparison, the 10 m result from Fig. 4 is also reproduced. Data from 13 December 2012 to 16 March 2013 (30 m and 10 m) and to 23 February 2013 (2 m).

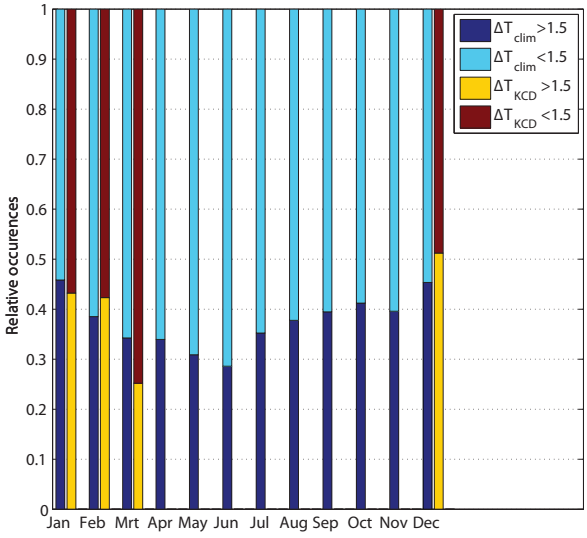

FIG. 9. Monthly climatology of ΔT_T for the years 2007-2011 (clim) and the period of KASCADE (KCD), the latter from December 2012 to March 2013.